

**Electronic Supplementary Material (ESI) for Nanoscale**  
**This journal is © The Royal Society of Chemistry 2013**

## **Supporting Information**

*for*

### **Multimodal chemo-magnetic control of self-propelling microbots**

Amit Kumar Singh<sup>a</sup>, Krishna Kanti Dey<sup>b</sup>, Arun Chattopadhyay<sup>a,c</sup>, Tapas Kumar Mandal<sup>d</sup> and  
Dipankar Bandyopadhyay<sup>\*a,d</sup>

<sup>a</sup>Centre for Nanotechnology, <sup>c</sup>Department of Chemistry, <sup>d</sup>Department of Chemical Engineering,  
Indian Institute of Technology Guwahati, Guwahati – 781039, India.

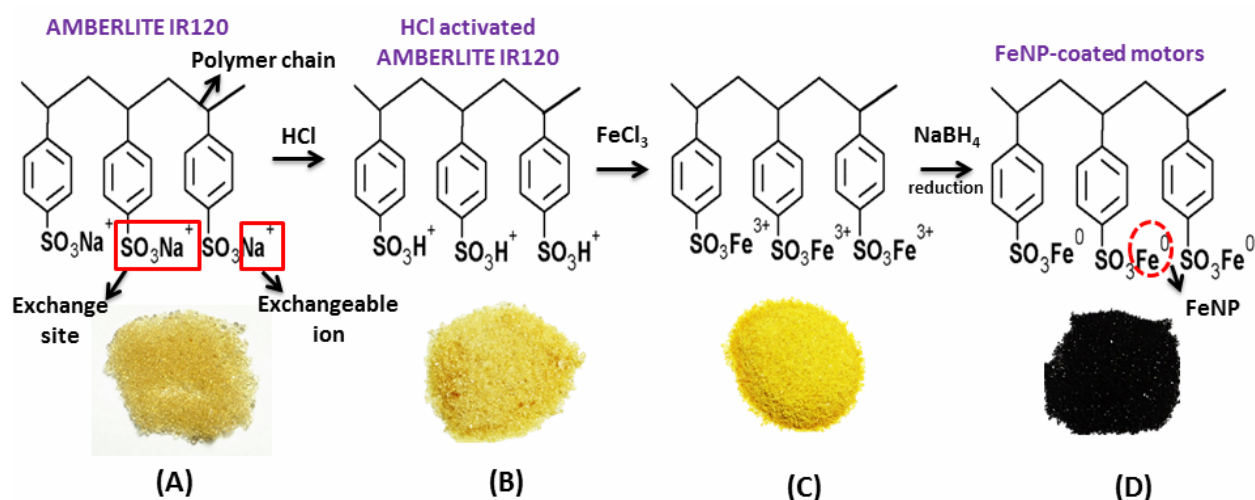
<sup>b</sup>Department of Chemistry,  
Pennsylvania State University, University Park, Pennsylvania- 16802, U.S.A.

\* *Corresponding author:* [dipban@iitg.ernet.in](mailto:dipban@iitg.ernet.in)

**Electronic Supplementary Material (ESI) for Nanoscale**  
**This journal is © The Royal Society of Chemistry 2013**

**Protocol for Depositing FeNPs on Polymer Resin Beads:**

The Amberlite IR 120 Na<sup>+</sup> beads are copolymers of styrene and di-vinyl-benzene, which has been sulfonated to produce a strong acid cationic resin, as shown in the image (A). The beads were crushed into fine particles of dimension 30 μm to 250 μm and cleaned 3-4 times with deionized water before air-dried on filter paper.



**Scheme 1.** Synthesis of iron nanoparticle (FeNP) coated polymer motors.

The washed beads were suspended in HCl (10 mL, 3.0 M) for 6 h at room temperature (25 °C) for activation. The activated beads are depicted in the image (B). Following this, the beads were washed thoroughly with water to remove excess HCl. Thereafter, the beads were suspended in FeCl<sub>3</sub>·6H<sub>2</sub>O solution (0.54 g dissolved in 10 mL C<sub>2</sub>H<sub>5</sub>OH) for 6 h at 25 °C and dried to the form as shown in the images (C). Following this, the particles were suspended in 5 mL of water and then NaBH<sub>4</sub> (5 mL of 0.66 M) was added drop-wise for 20 minutes with vigorous stirring. The particles were then filtered, washed, and vacuum dried. The black coloured beads in the image (D) were the FeNP coated motor after reduction.

Electronic Supplementary Material (ESI) for Nanoscale  
This journal is © The Royal Society of Chemistry 2013

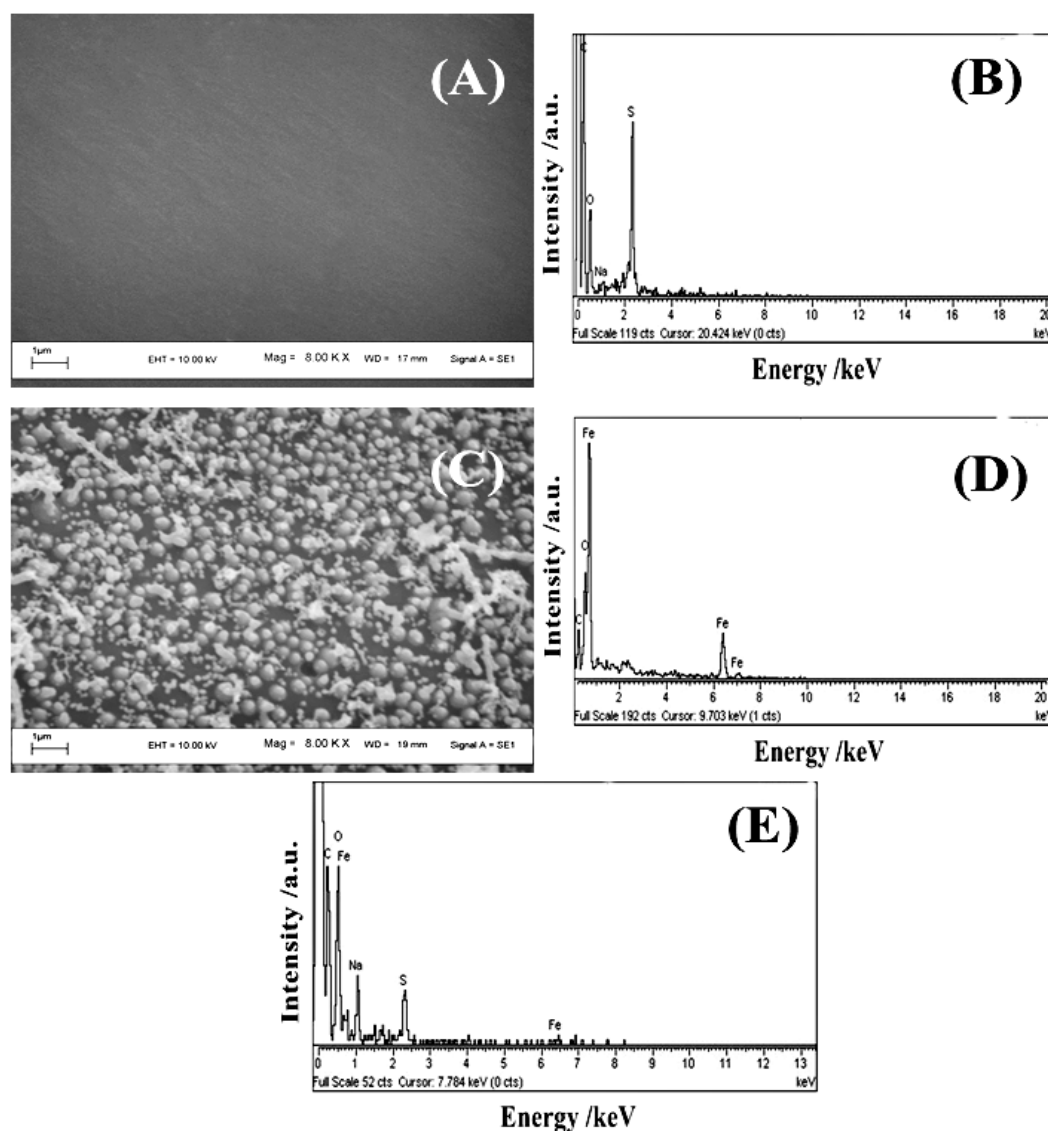


**Figure S1.** (A) Scanning electron microscopy (SEM) image of an uncoated polymer resin. The scale bar at the bottom is of 1  $\mu\text{m}$ . (B) Spot Energy Dispersive X-ray (EDX) of the uncoated polymer resin. (C) SEM image of a freshly prepared iron nanoparticle (FeNP) coated micromotor surface. FeNPs were observed in cluster-form, which was distributed over the motor surface. The scale bar at the bottom is of 1  $\mu\text{m}$ . (D) Spot EDX of FeNP coated micromotor shows the elemental Fe peak. (E) Spot EDX of FeNP coated micromotor after pre-treating with aqueous 9% (v/v) aqueous hydrogen peroxide for 30 minutes.

**Electronic Supplementary Material (ESI) for Nanoscale**  
**This journal is © The Royal Society of Chemistry 2013**

**Description of Figure S1**

The uncoated polymer resins and the freshly prepared FeNP coated polymer resins were characterized using LEO 1430VP scanning electron microscope, operating at a maximum voltage of 10 kV and at magnification of 8.0 kX. SEM image of a single FeNP deposited micromotor surface showed agglomerates of FeNPs<sup>1</sup> – size varying from 0.13  $\mu\text{m}$  to 0.50  $\mu\text{m}$  with an average of 0.27  $\mu\text{m}$  (**Figure S1 C**). The spot EDX on these agglomerates confirmed the presence of the FeNPs in the clusters (**Figure S1 D**). When the FeNP micromotor was treated with 9% (v/v) hydrogen peroxide solution for 30 min, the FeNPs were oxidized to iron oxide nanoparticles (FeO NPs) (**Figure S1 E**).

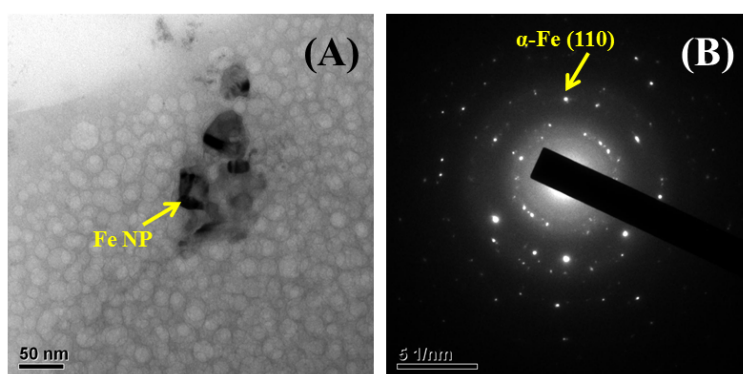


**Figure S2.** (A) Transmission electron microscopy (TEM) image of FeNP embedded in the polymer matrix. The scale bar at the bottom is 50 nm. (B) Selected area electron diffraction (SAED) pattern of a FeNP embedded in polymer matrix.

**Description of Figure S2**

The morphology of the FeNPs embedded in the amorphous polymer matrix were investigated by JEOL JEM 2100 Transmission electron microscope, operating at a maximum voltage of 200 kV. TEM images revealed that the FeNPs were 50 nm or less in size (**Figure S2 A**). The size observed in the SEM was of a cluster of FeNPs whereas the TEM image could further resolve the presence of smaller FeNPs in those clusters. The SAED pattern in the TEM showed a spotted sharp ring for d-spacing of 0.202 nm (calculated by DigitalMicrograph™ Software), which could be interpreted as body centred cubic structure for  $\alpha$ -Fe. The corresponding Miller indices for (110)  $\alpha$ -Fe is labelled on **Figure S2 B**.

Electronic Supplementary Material (ESI) for Nanoscale  
This journal is © The Royal Society of Chemistry 2013

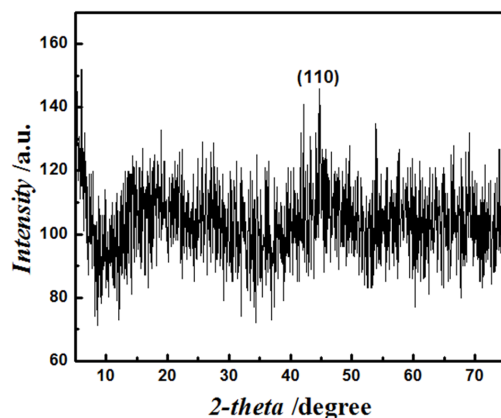


**Figure S3.** X-ray diffraction (XRD) of freshly prepared FeNP coated micromotor.

**Description of Figure S3**

The XRD of the freshly prepared FeNP coated micromotor showed a broad peak at  $2\theta = 44.8^\circ$ . The value was close to the body centred cubic  $\alpha$ -Fe for principal plane (110) at  $2\theta = 44.671^\circ$  (*JCPDS 06-0696*)<sup>2,3</sup> and was in agreement with the TEM results.

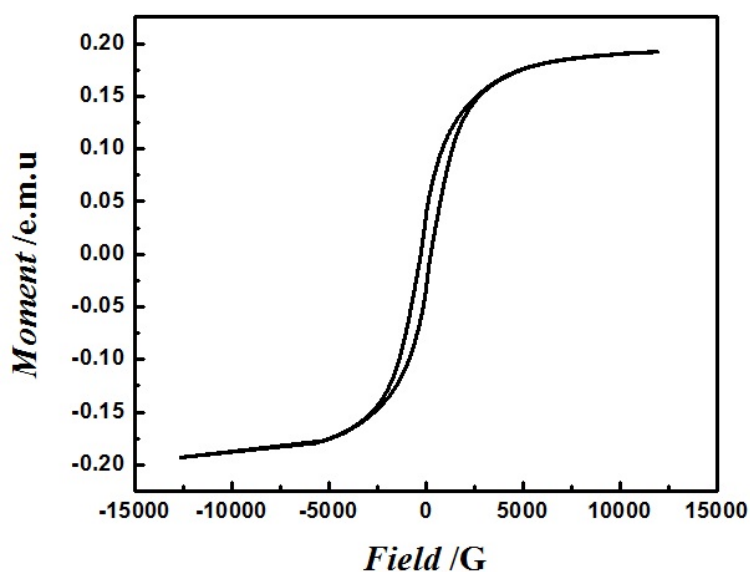


**Figure S4.** Vibrating sample magnetometry (VSM) hysteresis loop of freshly prepared FeNP coated micromotor.

**Description of Figure S4**

The magnetization curve was obtained from the VSM at  $25^\circ\text{C}$  by varying the magnetic field from  $-15$  to  $15$  kOe. The magnetization curve suggested that the FeNPs on the motor were soft ferromagnetic in nature.

Electronic Supplementary Material (ESI) for Nanoscale  
This journal is © The Royal Society of Chemistry 2013

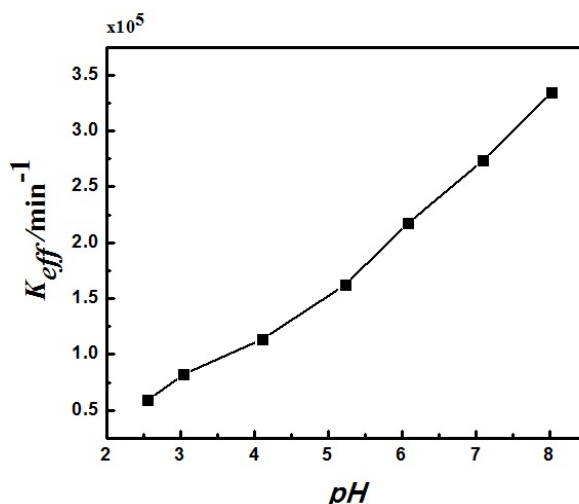


**Figure S5.** The variation in the effective rate constant ( $k_{eff}$ ) of hydrogen peroxide decomposition ( $\text{H}_2\text{O}_2$ ) with pH for a single catalytic micromotor.

### Description of Figure S5

The plot shows the variation in the effective rate constant ( $k_{eff}$ ) for the 9% (v/v) hydrogen peroxide ( $\text{H}_2\text{O}_2$ ) decomposition by a single catalytic motor at different pH. In presence of FeNP coated motor, the surface rate of decomposition of 9% (v/v)  $\text{H}_2\text{O}_2$  grew linearly with increase in the pH of  $\text{H}_2\text{O}_2$  bath (**Figure S5**).

### Description of Supporting Videos

#### (A) Supporting video 1

The video clip demonstrates the chemotaxis of a  $\sim 165 \mu\text{m}$  FeNP coated catalytic micromotor. The motor moved towards an alkali source under a pH gradient maintained by a NaOH supplier thread at the centre of a glass petridish. The pH gradient was tracked by phenolphthalein indicator, which turned from colourless to pink as the NaOH front moved from the centre to the sides of the glass petridish. The aqueous NaOH of known strength was continuously dripped from the reservoir to the bath in order to ensure that the pH was maintained higher (lower) near the thread (micromotor). The pH gradient produced a solute ( $\text{H}_2\text{O}_2$ ) concentration difference from the supplier thread to the micromotor by homogeneous catalytic decomposition of the solute ( $\text{H}_2\text{O}_2 \xrightarrow{\text{OH}^-} \text{H}_2\text{O} + 0.5\text{O}_2$ ) at different pH across the petridish. Furthermore, when the micromotor was placed inside the bath of peroxide fuel, the catalytic FeNPs on the motor surface started decomposing ( $\text{H}_2\text{O}_2 \xrightarrow{\text{FeNPs}} \text{H}_2\text{O} + 0.5\text{O}_2$ ) the solute through surface reaction and produced  $\text{O}_2$  bubble. The solute-motor interaction through the surface reaction created a local imbalance of solute

**Electronic Supplementary Material (ESI) for Nanoscale**  
**This journal is © The Royal Society of Chemistry 2013**

concentration across the motor, which was further magnified by the global gradient of the solute concentration. In consequence, the motor migrated towards the thread when the imbalance in solute-pressure owing to the solute concentration gradient across the motor surpassed the resisting viscous force<sup>4,5</sup>. The motor continuously depleted the solute while in motion towards the thread, which could be visualized through the emission of O<sub>2</sub> bubbles from the motor surface. The velocity of the motor away from the thread was found to be uniform at a lower pH gradient. In contrast, an accelerated motion was observed as the motor approached towards the thread<sup>5</sup>.

**(B) Supporting video 2**

The video shows that a ~165 μm FeNP deposited micromotor in a bath of 0.3M NaOH solution. The solution was devoid of H<sub>2</sub>O<sub>2</sub>. In this situation, no bubble formation was observed at the surface of the motor and the motor remained stationary during the course of observation. The video negates that the motion was due to the FeNP oxidation in alkaline solution and the bubbles issuing out were not composed of hydrogen gas.

**(C) Supporting video 3**

The video shows that when a ~165 μm FeNP deposited micromotor was placed inside a bath of 9% (v/v) aqueous peroxide fuel, the oxygen bubbles issued out from the surface of the motor to instigate a chaotic motion. The observation confirmed that the decomposition of peroxide on the surface was the primary reason behind the self-propulsion of the motor.

**(D) Supporting video 4**

The video clip demonstrates the activity of the ~190 μm micromotor under the pH gradient in absence of H<sub>2</sub>O<sub>2</sub>. In this case, the motor was introduced in a water bath and following this, aqueous 0.3M NaOH was continuously dripped from the reservoir to create the pH gradient. The motor was found to be stationary in this case. There was no issuance of bubble from the motor-surface during the experiment. The control experiment confirmed that the decomposition of peroxide was the prime reason behind the observed self-propulsion.

**(E) Supporting video 5**

In this experiment, the FeNP-coated micromotor was initially submerged inside 9% (v/v) aqueous H<sub>2</sub>O<sub>2</sub> solution for 15-20 minutes. Consequently, the FeNPs on the motor surface were pre-oxidized, as confirmed by the EDX in Fig. S1 E. Following this, we performed the migration experiment under the pH gradient with the motor having oxidized-FeNPs (FeO-NP) on the surface. The video

**Electronic Supplementary Material (ESI) for Nanoscale**  
**This journal is © The Royal Society of Chemistry 2013**

demonstrates that when a  $\sim 190$   $\mu\text{m}$  FeO-NP deposited micromotor moved towards the higher pH region in a 9% (v/v) peroxide bath when an aqueous 0.3M NaOH was continuously dripped. The experiment confirmed that the oxidation of the FeNPs on the motor surface did not significantly influence the directed chemotaxis.

**(F) Supporting video 6**

The video demonstrates that when a  $\sim 180$   $\mu\text{m}$  FeNP coated micromotor was introduced in alkaline 9% (v/v)  $\text{H}_2\text{O}_2$  bath of pH 6 and the alkali source at the same pH was continuously dripped into the bath, the motor did not show a directed motion. Instead it showed a vertical up and down motion owing to the change in the buoyancy originating from the periodic attachment or detachment of the oxygen bubbles on the surface. The oxygen bubbles were generated from the decomposition of peroxide fuel on the surface. The video confirms that in absence of the pH gradient although the motor showed catalytic activity but could not be directed. The experiment also corroborated the fact that the directed motion was not because of the simple mixing of peroxide and alkali.

**(G) Supporting video 7**

The video shows the controlled motion of  $\sim 190$   $\mu\text{m}$  catalytic micromotor while under an internal pH gradient. The motor could be promptly veered at different directions by placing the alkali source at different locations in the aqueous peroxide bath.

**(H) Supporting video 8**

The video clip shows the magnetic field induced motion of a  $\sim 165$   $\mu\text{m}$  FeNP coated catalytic micromotor. The motor migrated towards the applied external magnetic field. The imposed external magnetic field induced magnetism to the FeNPs deposited on the surface of the micromotor which in turn developed an attractive force between the motor and the magnetic pole to engender the motion. The motor continuously accelerated towards the magnetic pole as the magnitude of the magnetic attraction between the particle and the pole increased.

**(I) Supporting video 9**

The video clip demonstrates a controlled chemo-magneto taxis of a  $\sim 165$   $\mu\text{m}$  FeNP coated catalytic micromotor. The motor was initially set to a chemotactic motion towards the alkali dripping thread in which the pH gradient was indicated by the phenolphthalein indicator. Later, the movement of the motor was deviated with the help of an external magnetic field.



**Electronic Supplementary Material (ESI) for Nanoscale**  
**This journal is © The Royal Society of Chemistry 2013**

**(J) Supporting video 10**

The video clip demonstrates the control over the ~ 165  $\mu\text{m}$  FeNP coated catalytic micromotor as the motor was revolved around a thread (alkali source) in  $\text{H}_2\text{O}_2$  bath with the help of a rectangular bar magnet. The motor shows varying velocity as the bar magnet approaches and moves away from it while in motion around the thread.

**(K) Supporting video 11**

The video clip shows the reciprocating motion of a ~250  $\mu\text{m}$  micromotor inside a PDMS channel of width ~ 800  $\mu\text{m}$  under the coupled influence of the internal pH gradient and the external magnetic field. The motor moved towards the thread from a lower to higher pH region while it moved away from the thread in the opposite direction when migrated under the influence of an external magnet.

**(L) Supporting video 12**

The video shows a ~ 30  $\mu\text{m}$  catalytic micromotor hitting a cell cluster inside a microchannel (not visible due to higher magnification). The cells were placed between the thread supplying NaOH and the motor. The motor migrated towards the cell cluster (~ 170  $\mu\text{m}$ ) under the influence of the imposed pH gradient and hit the cell cluster, mimicking the action of a microscopic drug-delivery vehicle.

**References**

- [1] Z. Zongshan, L. Jingfu, T. Chao, Z. Qunfang, H. Jingtian and J. Guibin, *Sci. China Chem.*, 2008, **51**, 186.
- [2] Z. Jiang, L. Lv, W. Zhang, Q. Du, B. Pan, L. Yang and Q. Zhang, *Water Res.*, 2011, **45**, 2191.
- [3] X. Cheng, B. Wu, Y. Yang and Y. Li, *Catalysis Comm.*, 2011, **12**, 431.
- [4] J. F. Brady, *J. Fluid Mech.*, 2011, **667**, 216.
- [5] K. K. Dey, S. Bhandari, D. Bandyopadhyay, S. Basu and A. Chattopadhyay, *Small*, 2013, **9**, 1916.